APPENDIX A

"Network Models of Coal Thermal Decomposition"

Paper Submitted to Fuel

NETWORK MODELS OF COAL THERMAL DECOMPOSITION

Peter R. Solomon, David G. Hamblen, Zhen-Zhong Yu, and Michael A. Serio

Advanced Fuel Research, Inc., 87 Church Street, East Hartford, CT 06108

ABSTRACT

Several groups have considered statistical network fragmentation models to describe coal thermal decomposition. In these models, the coal macromolecule is viewed as a collection of fused aromatic rings (monomers) linked by bridges. During thermal decomposition, existing bridges break and new bridges are formed. The parameters of the models are the geometry of the network, which is expressed as the number of attachments per monomer (the coordination number, $\sigma+1$), and the chemistry of bridge breaking and formation. Given σ and the instantaneous number of unbroken and formed bridges, the molecular weight distribution can be predicted. The different groups have employed both Monte Carlo methods and percolation theory to describe the network statistics. The latter approach has advantages in terms of describing both the depolymerization and crosslinking processes in coal decomposition, since it does not require a constant coordination number, although is computationally more intensive. The models differ in the geometry of the network, the chemistry of bridge breaking and bridge formation (crosslinking) and the mass transport assumptions. This paper considers: a) the mathematical schemes; b) the assumed geometries (σ's); c) the assumed bond breaking and bond formation chemistries, and d) the mass transport assumption for three such models. A comparison of the predictions of three models was made by comparing the oligomer populations as a function of the number of unbroken bridges per ring cluster. The paper presents results from a new model which combines the geometry, chemistry and mass transport assumptions of our FG-DVC model with the mathematics of a modified percolation theory.

NETWORK MODELS OF COAL THERMAL DECOMPOSITION

Peter R. Solomon, David G. Hamblen, Zhen-Zhong Yu, and Michael A. Serio

Advanced Fuel Research, Inc., 87 Church Street, East Hartford, CT 06108

INTRODUCTION

Many recent studies have proposed that coal can be thought of as having a macromolecular network structure to which concepts of crosslinked polymers can be applied.[1-10] These concepts have been employed to understand and model such properties of coal as: i) the insolubility; ii) the equilibrium swelling and penetration of solvents; iii) the viscoelastic properties; iv) similarities between the parent coal and products of hydrogenolysis, or mild oxidation; v) crosslinking during char formation[11,12]; and vi) the formation of coal tar in pyrolysis.[13-17] With the success of these concepts in describing coal properties, it appears logical to extend macromolecular network concepts to completely describe coal thermal decomposition behavior.

A number of investigators have applied statistical methods to predict how the network behaves when subjected to thermally induced bridge breaking, crosslinking, and mass transport processes.[17-20] Gavalas et al. employed statistical methods to predict the release of monomers from a randomly connected network.[20] The model of Niksa and Kerstein employed percolation theory in a model called DISARAY[28] which extended their previous model built on chain statistics.[24,25] Grant et al. employed percolation theory in a model called Chemical Percolation Devolatilization (CPD).[30] Solomon et al. employed Monte Carlo methods in a network model called the Depolymerization, Vaporization, and Crosslinking (DVC) model.[21-23,27] This was an extension of their previous model for linear polymers.[17,29] The DVC model was recently combined with their Functional Group (FG) model[27,29] to produce the general FG-DVC pyrolysis

model. This model is currently being applied to model the devolatilization behavior of the Argonne premium coals[31] and to predict the fluidity of coals.[32] Other statistical methods for network behavior have been employed in the polymer literature.[33-38]

In applying network models to coal thermal decomposition, one considers the coal to consist of aromatic ring clusters linked together by bridges in some geometry. When the coal is heated, the bridges can break and new bridges can form. Various statistical methods can be employed to predict the concentration of single aromatic ring clusters (monomers) and linked clusters (oligomers of n clusters, "n-mers") up to a totally linked network. By assigning an average or distribution of molecular weights to the monomers, the amounts of tar, extractables, liquids or char can then be defined from the distribution of oligomer sizes. The models vary in the assumed chemistry of bridge breaking and crosslinking, in the definition of tar, extracts, liquids, and char and in the statistical methods used.

In view of the importance of macromolecular network models to the accurate predictions of coal processing behavior, this paper assesses the assumptions and limitations of the proposed models. It appears that the way one performs the statistics (Monte Carlo, percolation theory, or other statistical methods) makes little difference. For example, we have substituted percolation theory methods for Monte Carlo calculations in the FG-DVC model and obtained comparable predictions for appropriately restricted cases. The important differences among models are in the assumptions for: 1) the network geometry; 2) the chemistry of bridge breaking; 3) the chemistry of crosslink formation; 4) hydrogen utilization; and 5) mass transport. The paper compares the three most recent models (DISARAY, CPD, and FG-DVC) and considers how the assumed network properties relate to behaviors observed for coal.

MACROMOLECULAR NETWORKS

General Properties of Networks

Figures 1 and 2 present the networks employed in the FG-DVC Monte Carlo calculations and percolation theory, respectively. For the FG-DVC Monte Carlo calculation, oligomers of t clusters (shown as the horizontal chains of clusters) of a molecular weight distribution defined by M_{avg} and deviation, ΔM, are linked by m_o crosslinks per monomer (shown as the vertical double lines).[28,29] The crosslinks are the branch points in the network where more than two bridges connect a cluster. During thermal decomposition, bridges break, crosslinks are added and the molecular weight of the oligomers is calculated by randomly distributing these changes.

For the percolation theory, a Bethe lattice is employed.[25,30,39] Lattices are characterized by the coordination number, $(\sigma + 1)$, which is the number of bridges sites per cluster and the probability, p, that an unbroken bridge occupies the site. Figure 2 shows lattices for $\sigma + 1 = 2.2$ and $\sigma + 1 = 4$. The Bethe lattice has no loops, but it has been demonstrated that this lattice is a good approximation to a lattice of equivalent coordination number containing loops.[39]

The loop free geometry of the Bethe lattice allows for the number of free oligomers to be analytically expressed as a function of σ and the probability p of bonds being unbroken. This is the feature which makes the percolation theory so attractive from the standpoint of computer efficiency and for understanding the behavior of networks under conditions of varying bridge populations. In Fig. 3, we present calculations using percolation theory (for three values of $\sigma + 1$) for the monomer, the sum of oligomers up to 3, up to 10, and the sum of all free oligomers as a function of the number of unbroken bonds per ring cluster α, where

- - -

$\alpha = 1/2\,p\,(\sigma + 1)$. If σ remains constant during pyrolysis, the molecular weight distribution is a single valued function of α. For ring clusters of molecular weight 300 amu, the sum of 1 to 3 n-mers corresponds roughly to the potential tar fraction (up to 900 amu), the sum of 1-10 n-mers corresponds to the extractable fraction (up to 3000 amu), and the sum of all oligomers corresponds to the liquids fraction (all free oligomers). It can be seen that, with increasing σ, more broken bonds are required to achieve equivalent fractions of free oligomers. Also, at a fixed value of α, the relative amounts of tar, extracts, and liquids vary with σ.

Network Geometries Representative of Coal

The three important parameters of the network are the average ring cluster size M_{avg}, the coordination number $(\sigma + 1)$, and the starting probability of bridges being unbroken, p_o. For comparing networks of different coordination numbers, it is convenient to use α rather than p. The assumptions of DISARAY, CPD, and FG-DVC are considered below.

Ring Cluster Size - Ring cluster sizes have been estimated from NMR alone,[40] NMR and FT-IR,[41] mild degradation,[42] and the molecular weight distribution of tar.[15,16,29] Based on these results, the average ring cluster size for coals with less than 90% carbon is expected to be between 2 and 3 aromatic rings or a total molecular weight per cluster, including peripheral groups, of 200-400 amu.

DISARAY assumes a value of 1400 amu for the monomer which can split into two 700 amu tar fragments. CPD does not specify the monomer molecular weight. For coals with less than 90% carbon, FG-DVC employs a distribution of monomers with an M_{avg} of 256 amu.

Coordination Number - Information on the coordination number comes from estimates from solvent swelling measurements of the average molecular weight between crosslinks,

M_c,[2-9] and recent estimates made using NMR of the number of non-peripheral group attachments to the cluster.[40] The M_c determinations suggest that there are between 4 and 8 repeating units between crosslinks (or branch points). This indicates a value for $\sigma + 1$ between 2.13 and 2.25. The NMR data suggest that there are between 2 and 3 bridge or loop attachments per cluster (see Fig. 8 of Ref. 40). This suggests $\sigma + 1$ is between 2 and 3. Based on these two above measurements, the coordination number for the starting coal for describing the break up of the network by bridge cleavage should be less than 3, and probably between 2.2. and 2.5. A different value of $\sigma + 1$ might be appropriate for describing crosslinking, as discussed later.

To model a high volatile bituminous coal, the different models used networks with $(\sigma + 1) = 3.25$ (DISARAY), 4.6 (CPD), and ≈ 2.1 (FG-DVC).

Initial Bond Population - The starting macromolecular network for FG-DVC is chosen to match the measured extract yield and molecular weight between crosslinks by picking two parameters: i) the length of the oligomer chain, ℓ, ii) the number of initial crosslinks per monomer, m_o. First m_o is picked such that $m_o = M_{avg}/M_c$ where M_{avg} is the average monomer molecular weight and M_c is the molecular weight between crosslinks determined from solvent swelling.[2-9] Then ℓ is chosen so that when the molecule is randomly constructed, the weight percent of oligomers less than 3000 amu matches the measured extract yield. There is the implicit assumption that the extract yield is due to the unpolymerized fraction of a homogeneous network. Polymethylenes or highly fluid macerals (e.g., exinites), which can be a significant portion of the extracts in coal, should really be treated as separate components but were not in the first version of the FG-DVC model. The initial value of α is approximately $((\ell - 1)/\ell + m_o)$, which for the Pittsburgh Seam coal modeled in Ref. 29 is $\alpha_o \approx 0.95$. This initial value is indicated in Fig. 3a.

In DISARAY, p_o is set equal to 1 (α_o = 1.63). This is illustrated in Fig. 3b.

The starting macromolecular network in the CPD model is chosen by picking two parameters: i) the coordination number σ + 1, picked to match the average number of attachments **(bridges and peripheral groups)** per ring determined by NMR;[30,40] and ii) p_o the starting probability of unbroken bonds. For the high volatile bituminous coal simulated in Ref. 30, α_o = 1/2 p_o (σ ÷ 1) = 1.36. This initial value is indicated in Fig.3c.

PROCESSES CONTROLLING THE NETWORK DECOMPOSITION

This section considers the important processes in pyrolysis: bridge breaking, and hydrogen utilization; crosslinking; and the mass transport processes which control the distribution of oligomers into tar, extracts, liquids, and solids. The processes are summarized in Fig. 4.

Bridge Breaking and Hydrogen Utilization

Figure 4a summarizes the bridge breaking assumptions of the three models. Both the FG-DVC and CPD models assume similar (within a factor of 3) bridge breaking rates, 0.86×10^{15} exp-(55,400/RT) sec^{-1} for FG-DVC* and 2.6×10^{15} exp-(55,400/RT) sec^{-1} for CPD. Both models employ rank independent kinetics. The FG-DVC model rate was determined in experiments in which particle temperatures were directly measured.[43] The rate was recently confirmed within a factor of 2 by Fletcher et al. in a second experiment which directly measures particle temperatures.[44] The DISARAY model assumes a bridge dissociation rate of 6×10^8 exp-(30,000/RT) sec^{-1}* which can produce monomers. The monomers subsequently decompose at 1.4×10^7 exp-(-31,000/RT) sec^{-1} to form tar.

In DISARAY, all the initial bridges can break. In FG-DVC and CPD, there is a process for creating unbreakable bridges associated with the bridge breaking process. The FG-DVC model includes three kinds of bonds: labile bridges, unbreakable bridges, and crosslinks. For each broken labile bridge, FG-DVC requires that hydrogen be available to stabilize the free radicals. It is assumed that all the donatable hydrogen (aliphatic plus hydroaromatic) is located in the labile bridges, so that only half the labile bridges can break with the other half becoming unbreakable with the donation of their hydrogen (i.e., there is a 1:1 ratio between the occurrence of bridge breaking and the formation of additional unbreakable bridges). The weight fraction of the initial bridges in the chain of length ℓ which are labile is given by the parameter W_B; the rest are assumed to be unbreakable bridges. W_B is a fitting parameter chosen to make the model fit the pyrolysis data.

In a similar manner, in CPD there are both unbreakable bridges with probability c_o and labile bridges with probability ℓ_o ($\ell_o + c_o = p_o$). As pyrolysis proceeds, the labile bridges can break and react by two possible routes to form unbreakable "char" bridges or broken bridges. CPD assumes a 0.9:1.0 ratio for the ratio of broken bridge to char bridge formation. That assumption is almost identical to the 1:1 ratio used in FG-DVC.

Crosslinking

The crosslinking reactions are summarized in Fig. 4b. CPD does not assume any crosslinking processes except those char forming reactions occurring as a consequence of bridge breaking (discussed above).

* both FG-DVC and DISARAY employ distributed activation energy expressions. The rates quoted above are for the center of the distribution.

DISARAY assumes char formation occurs at a rate $2 \times 10^6 \exp{-(24,600/RT)}$ sec^{-1}. Char formation is assumed to occur by monomers attaching to the original lattice or to each other.

FG-DVC assumes two independent crosslinking reactions in addition to the unbreakable bridge formation accompanying hydrogen donation. One occurs at low temperature (below that for bridge breaking) for low rank coals and is associated with CO_2 evolution.[11,12,45] Crosslinking also occurs at moderate temperatures, slightly higher than bridge breaking, and is associated with the evolution of CH_4. The model assumes one crosslink is formed for each CH_4 or CO_2 evolved.[29] The mechanistic basis for these assumptions has been discussed elsewhere.[45]

Product Distribution

The product distribution assumptions are summarized in Fig. 4c. The identification of different size oligomers with tar, extracts, liquids, and solids is related to their molecular weight. The oligomers which can form tar are the lightest fraction. Tar formation is controlled in part by the vapor pressure of the components. This idea is supported by the observation that tar yields are strongly influenced by external pressure.[29,46,47]

Only oligomers with molecular weights less than 1000 amu have sufficient vapor pressure to become gas at typical pyrolysis temperatures, so tar is roughly limited to < 1000 amu.[47-51] The extract yield is controlled by the solubility of the oligomers. For coal fragments in pyridine this limit is roughly 3000 amu.[47-49,52] Larger fragments appear to be important to the fluid properties of coal.[32]

In FG-DVC, the Monte Carlo calculation is employed to determine the molecular weight distribution in the decomposing char. Then, a mass transport equation is applied to determine

the probability of the light n-mers evolving as tar. The transport equation assumes that a molecular weight dependent vapor pressure controls the appearance of these molecules in the gas phase and that they escape the coal particles by convective transport of the gas.[29] Tar is thus the light end of the molecular weight spectrum, i.e., those with sufficiently high vapor pressures. This produces tar with number average molecular weights of 300-400 amu and maximum weights of 800-1000 amu. Thus, in FG-DVC, tar is approximately the sum of 1-3 n-mers in Fig. 3a. Extractable material is defined as all molecules up 3000 amu (sum of 1-10 n-mers) and liquids are defined as all molecules not attached to the starting network.

In DISARAY, tar is defined as half the monomer, and the monomer is taken as 1400 amu. Consequently, the tar would be defined as some fraction of the monomer curve in Fig. 3b.

No transport equations are employed in CPD. Tar is defined as all molecules not attached to the infinite lattice. Thus tar is represented by the highest line in Fig. 3c.

One advantage of the Monte Carlo method over the percolation theory is that, when tar is produced, molecules can be removed from the network. In percolation theory, there is no mechanism for removing molecules from the network. If there are crosslinking events, as in FG-DVC, all the small molecules can reconnect to the network. CPD avoids this problem by excluding any independent crosslinking which would reconnect oligomers. This presents the limitation that independent crosslinking and mass transport cannot be treated with the exact percolation theory expressions.

EXAMPLES OF MODEL CALCULATIONS

Formation of Pyrolysis Products

The evolution of the macromolecular network in the CPD model is illustrated in Fig. 5. Figure 5a shows the percolation theory predictions for the total of unattached oligomers (defined to be the tar) as a function of α. The coal is represented at $p_0 = 0.59$ or $\alpha_0 = 1/2\, p_0\, (\sigma + 1) = 1.36$. During pyrolysis, the labile bridges form either broken bridges or unbreakable char bridges in the ratio 0.9 to 1.0. Figure 5b shows how α changes during pyrolysis. Pyrolysis proceeds until α_{min} is reached where all the labile bridges are either broken or have formed unbreakable bridges. Thus

$$\alpha_{min} = 1/2\, (\sigma + 1)\, (c_0 + (1.0/1.9)\alpha_0^{\prime}) = 0.83$$

and the change in α during pyrolysis was 0.53.   Note that α only decreases in the CPD model.

The evolution of the macromolecular network for FG-DVC computed using the Monte Carlo method for a bituminous coal is illustrated in Fig. 6. Figure 6a shows the calculated extract yield as a function of α. The initial probabilitv of unbroken bridges, α_0, starts out at close to 1.0 to produce the measured extract yield (30%). Figure 6b shows the computed value of α with its contributions from the initial crosslinks m_0, the conversion of labile bridges to broken bridges and unbreakable bridges and the added crosslinks related to gas evolution. For the bituminous coal, the added crosslinks are almost all due to CH_4 related processes. Note that α goes back up in the FG-DVC model to resolidify the lattice. This is necessary to model fluidity effects.[32]

Results of the FG-DVC model applied to a lignite are presented in Fig. 7. For the lignite, the formation of low temperature crosslinks from CO_2 evolution prevents α from being reduced due to bridge breaking. Thus pyrolysis produces no additional extract yield. The low rank coals in being thermosetting and releasing little tar or extracts is related to this low temperature crosslinking process.

Utilization of Donatable Hydrogen

As discussed above, W_B, the initial fraction of labile bridges, is a parameter of the FG-DVC model. This parameter is related to the fraction of donatable hydrogen by $H(d) = 2/28\ W_B$; i.e., there are two donatable hydrogens per labile bridge. This parameter has a strong effect on α_{min} and hence the yield of tar, extracts, and liquids.

There are two ways to estimate the amount of hydrogen donated. During pyrolysis, the donation of hydrogen converts two aliphatic or hydroaromatic hydrogens into a donated aliphatic hydrogen plus a newly formed aromatic hydrogen. We can measure both the increase in aromatic hydrogen in the pyrolysis products and the increase in aliphatic hydrogen in the tar using quantitative FT-IR analysis.[53,54] The results for a Pittsburgh Seam coal are summarized in Fig. 8. They show that the aromatic hydrogen in the total pyrolysis products increased from 2.1 to 2.4%, or an increase of 0.3% on a starting coal basis. This increased aromatic content is all in the char. The aromatic content in the tar remains about the same. The tar, which is approximately 30% of the starting coal, increases its aliphatic hydrogen content by about 1% o 0.3% on the starting coal basis. The two numbers are thus consistent; 0.6% donatable hydrogens in the coal are converted to 0.3% new aromatics plus 0.3% donated aliphatics. If it is assumed that a monomer has a molecular weight of 300 amu, then one breakable bridge per monomer with four aliphatic hydrogens is 1.33% donatable hydrogen. Half the bridges can break (0.67%) and the other half can donate hydrogen (0.67%), in reasonable agreement with

the experimentally estimated value of 0.6% hydrogens actually donated. The value assumed in FG-DVC for H(d) for the Pittsburgh Seam coal is 0.67%.[29]

The value of H(d) has implications for the CPD model. If there is only one labile bridge per monomer, then

$$\alpha_{min} = 1/2 \ (\sigma + 1) \ (C_o + (1.0/1.9)\chi_o) = 1/2 \ (4.6) \ (0.37 + (1.0/1.9) \ 0.22) = 1.11$$

rather than 0.83. In this case, the value of $\sigma + 1$ would have to be reduced to match the data. Also, the average molecular weight for the unattached molecules is too high to be identified as tar. If a more reasonable definition of tar is used (e.g., the sum of oligomers up to 3), then $\sigma + 1$ would have to be reduced still further.

Comparison of Monte Carlo Calculation with Percolation Theory

To further illustrate some of the differences between the FG-DVC Monte Carlo model and percolation theory calculations, the extract yield calculated for a case similar to that in Fig. 6a, but with tar evolution not permitted is plotted in Fig. 9 along with the predictions of percolation theory for several values of α. The FG-DVC Monte Carlo prediction is not a single valued function of α. As pyrolysis proceeds, the increase in extract yield follows $\sigma + 1 \approx 2.2$ while the decrease in extract yield follows $\sigma + 1 \approx 4$.

It is important to know whether this result is an artifact of the Monte Carlo calculation or a real feature of pyrolysis. Based on what is known to happen in pyrolysis, the result does make sense. For a bituminous coal, the initial process occurring in pyrolysis is bridge breaking. This occurs by breaking bridges in the network described by $\sigma + 1$ between 2.1 and 2.5. No crosslinking is occurring initially as the solvent swelling ratio is observed to increase

during this period.[45] Eventually crosslinks start forming, resulting in an increase in the coordination number and in α. Consequently, the network cannot adequately be described by one type of bridge site with a single coordination number. There are bridge sites for labile bridges and for crosslinks, each with their own coordination number. This observation motivated the development of a more general percolation theory model, discussed below.

LATTICE MODEL WITH TWO BRIDGE BOND TYPES

Two-σ Model - In order to deal with a structure with a time dependent coordination number, we consider a Bethe lattice with two types of bridging bonds, with coordination numbers and probabilities of occupation given by $\sigma_1 + 1$, p, and $\sigma_2 + 1$, q, for the two types, respectively. Such a lattice for $\sigma_1 = \sigma_2 = 1$ is illustrated in Fig. 10. The analysis can be carried through using the same procedures as Fisher and Essam [33] or Ref. 30, but with extensions to deal with the extra variables. The equations are presented in the Appendix.

Application of Two-σ Model - Figure 11 presents a comparison of the predictions for pyrolysis assuming the FG-DVC chemistry using: a) the Monte Carlo calculation, b) the two-σ percolation calculations ($\sigma_1 = 1$, $\sigma_2 = 1$) and c and d) two cases of the one-σ percolation calculation ($\sigma = 2.2$ and $\sigma = 3.2$). The calculations are made under the assumption that no tar is evolved. The tar values in Fig. 11 are the sum of 1-3 n-mers remaining in the char. The Monte Carlo calculation in Fig. 11a is matched best by the two-σ model if liquids are assumed to be the sum of the first 100 n-mers (i.e., up to 300,000 amu). The two-σ model has a reasonable value for the initial extract yield but predicts slightly more initial tar. Neither of the one-σ cases is a good match. Use of $\sigma = 2.2$ is good at low temperature, but overpredicts the maximum values of extracts and liquids. Use of $\sigma = 3.2$ does a much better job on predicting the maximum values, but the initial ratio of tar to extract is not consistent with what is observed for coal and the rate of increase of n-mers is too slow. It thus appears that the two-σ model

can be used instead of the Monte Carlo calculations when no tar is evolved, while one-σ calculations are less accurate.

The real test, however, is how well the models fit the data for coal. A comparison of tar yield is not a sufficient test since α_o and $\Delta\alpha$ can always be selected in conjunction with the network geometry to fit the data. A critical test requires a careful comparison of how α_o and $\alpha(t)$ match with measurement of functional group changes in the char (e.g., the transformation of hydrogen functional groups and bridges), solvent swelling behavior (i.e., crosslink density), and the complete molecular weight distribution as reflected in the amounts of tar, extracts, and fluidity.

COMPARISON OF NETWORK MODELS

A summary of the processes predicted by the three recent network models, CPD, DISARAY and FG-DVC is presented in Table I. All the models predict their primary objective, the variations in tar and gas yield with time and temperature. All three are capable of predicting variations of tar yield with heating rate, but CPD has not yet done this. All three models are capable of predicting the complete molecular weight distributions of fragments, but only FG-DVC uses this information to predict the extract yield, the tar yield and the tar molecular weight distribution. DISARAY uses only the prediction for monomers (defined as tar precursor) and CPD uses only the prediction for all oligomers (defined as tar). In a recent paper, the total oligomer population computed by the FG-DVC model is used to predict coal fluidity behavior.[32] Only FG-DVC employs a mass transport equation which is necessary to predict tar molecular weights and the variations of yield and molecular weights with pressure. Only FG-DVC predicts the solvent swelling ratio, which is determined by the crosslink density in the char.

CONCLUSIONS

1) The extension of macromolecular network concepts to describe coal thermal decomposition appears to be very successful and versatile in allowing the prediction of tar, extract yield, and total liquids.

2) A complete model requires a description of: i) labile bridge breaking with hydrogen utilization; ii) rank dependent crosslinking processes; and iii) mass transport.

3) Monte Carlo methods for computing the network statistics are the most versatile, but are computationally demanding.

4) The use of percolation theory is computationally efficient and helps provide insight into network behavior, but the use of a fixed coordination number may be inadequate to accurately describe coal thermal decomposition. The network appears to require a coordination number between 2.2 and 2.5 during labile bridge breaking and greater than 3 during crosslinking, if a single type of bridge site is assumed.

5) Alternatively, a more general percolation theory model for a network with two types of bridging bonds was developed, each with their own σ.

6) When the two-σ percolation model is applied using the FG-DVC chemistry to cases in which tar is not removed, it gives results which are comparable to the Monte Carlo calculation. Applying percolation theory to cases where tar is removed requires additional approximations.

7) Of the three models which were compared (CPD, DISARAY, and FG-DVC), FG-DVC is the most complete in treating the molecular weight of network fragments and the processes of vaporization and mass transport to define tar, the tar molecular weight distribution and the extract yield.

8) Of the three models, FG-DVC is the most closely related with the previous concepts of coal as a macromolecular network by requiring that the network predict the coal, char solvent swelling ratios, and measured extract yields. The assumptions which define the parameters of the starting network are open to question and must be explored.

9) Future effort should focus on identifying the chemistry for the processes of bridge breaking, low temperature crosslinking, moderate temperature crosslinking, and hydrogen utilization.

ACKNOWLEDGEMENT

REFERENCES

1. Van Krevelen, D.W., Coal, Elsevier, Amsterdam, (1961).

2. Green, T.K., Kovac, J., and Larsen, J.W., Fuel, (1984), 63, 935.

3. Brenner, D., Fuel, (1985), 64, 167.

4. Lucht, L.M. and Peppas, N.A., Fuel, (1987), 66, 803.

5. Lucht, L.M., Larsen, J.M., and Peppas, N.A., Energy & Fuels, (1987), 1, 56.

6. Larsen, J.W., ACS Fuel Chem. Div. Preprints, (1985), 30, (4), 444.

7. Green, T., Kovac, J., Brenner, D., and Larsen, J., Coal Structure, (R.A. Meyers, Ed.),
   Academic, NY, (1982), p 199.

8. Hall, P.J., Marsh, H., and Thomas, K.M., Fuel, (1988), 67, 863.

9. Sanada, Y. and Honda, H., Fuel, (1966), 45, 295.

10. Suuberg, E.M., Yoshi, O., and Deevo. S., ACS Div. Fuel Chem. Prepr., (1988), 33, (1), 387.

11. Suuberg, E.M., Lee, D., and Larsen, J.W., Fuel, (1985), 64, 1668.

12. Suuberg, E.M., Unger, P.E., and Larsen, J.W., Energy & Fuels, (1987), 1, 305.

13. Brown, J.K., Dryden, I.G.C., Dunevein, D.H., Joy, W.K., and Pankhurst, K.S., J. Inst. Fuel,
    (1958), 31, 259.

14. Orning, A.A. and Greifer, B., Fuel, (1956), 35, 318.

15. Solomon, P.R. and Hamblen, D.G., Chemistry in Coal Conversion, (R.H. Schlosberg, Ed.),
    Plenum, New York, (1985), p. 121, Chapter 5.

16. Solomon, P.R., New Approaches in Coal Chemistry, ACS Symposium Series 169, ACS,
    Washington, DC, (1981). p. 61.

17. Solomon, P.R., and King, H.H., Fuel, (1984), 63, 1302.

18. Gavalas, G.R., Coal Pyrolysis, Elsevier, NY, (1982), p. 51.

19. Gavalas, G.R., Cheong, P.H., and Jain, R., Ind. Eng. Chem. Fundam., (1981), 20, 122.

20. Squire, K.R., Solomon, P.R., Carangelo, R.M., and DiTaranto, M.B., Fuel, (1986), 65, 833.

21. Squire, K.R., Solomon, P.R., DiTaranto, M.B., and Carangelo, R.M., ACS Div. of Fuel Chem.
    Preprints, (1985), 30, (1), 386.

22. Solomon, P.R., Squire, K.R., and Carangelo, R.M., Proceedings of the Int. Conf. on Coal
    Science, Pergamon, Syndey, Australia, (1985), p. 945.

23. Solomon, P.R., and Squire, K.R., ACS Div. of Fuel Chem. Preprints, (1985), 30, (4), 347.

24. Niksa, S., and Kerstein, A.R., Combustion and Flame, (1986), 66, 95.

25. Niksa, S., Combustion and Flame, (1986), 66, 111.

26. Solomon, P.R., Hamblen, D.G., Deshpande, G.V. and Serio, M.A., A General Model of Coal Devolatilization, Proceedings of the International Coal Science Conference, Elsevier, NY, (1987), p. 601.

27. Solomon, P.R., Hamblen, D.G., Carangelo, R.M., Serio, M.A., and Deshpande, G.V., Combustion and Flame, (1988), 71, 137.

28. Niksa, S. and Kerstein, A.R., Fuel, (1987), 66, 1389.

29. Solomon, P.R., Hamblen, D.G., Carangelo, R.M., Serio, M.A. and Deshpande, G.V., Energy and Fuels, (1988), 2, 405.

30. Grant, D.M., Pugmire, R.J., Fletcher, T.H., and Kerstein, A.R., Energy & Fuels, (1989), 3, 175.

31. Serio, M.A., Solomon, P.R., Yu, Z.Z., Deshpande, G.V., and Hamblen, D.G., ACS Div. of Fuel Chem. Preprints, (1988), 33, (3), 91.

32. Solomon, P.R., Best, P.E., Yu, Z.Z., and Deshpande, G.V., "A Macromolecular Network Model for Coal Fluidity", ACS Div. of Fuel Chem. Preprints, 34, paper presented at the Miami ACS meeting, (9/1989).

33. Nielsen, L.E., Mechanical Properties of Polymers and Composites, Vol. 2, Marcel Dekker, Inc. NY, (1974).

34. Bartels, C.R., Crist, B., Felters, L.J., and Graessley, W.W., Macromolecules, (1986), 19, 785.

35. Nazem, F.F., Fuel, (1980), 59, 851.

36. Macosko, C.W., Brit. Polymer Journ., (1985), 17, 239, and references therein.

37. Flory, P.J., J. Am. Chem. Soc., (1941), 63, 3083, 3097; see also Principles of Polymer Chemistry, Cornell University Press, Ithaca, NY, (1953), Chapter 9.

38. Stockmayer, W.H., J. Chem. Phys., (1943), 11, 45; also (1944), 12, 125.

39. Fisher, M.E., and Essam, J.W., J. Math. Phys., (1961), 2, 609.

40. Solum, M., Pugmire, R.J., and Grant, D.M., Energy & Fuels, (1989), 3, 40.

41. Gerstein, B.C., Murphy, D.P., and Ryan, L.M., Coal Structure, (R.A. Meyers, Ed.), Academic Press, NY, (1982), p. 87, Chapter 4.

42. Hooker, D.T., II, Lucht, L.M., and Peppas, N.A., Ind. Eng. Chem. Fundam., (1986), 25, 103.

43. Solomon, P.R., Serio, M.A., Carangelo, R.M., and Markham, J.R., Fuel, (1986), 65, 182.

44. Fletcher, T.H., Combustion Science and Technology, (1989), 63, 87.

45. Deshpande, G.V., Solomon, P.R., and Serio, M.A., ACS Div. of Fuel Chem. Preprints, (1988), 33, (2), 310.

46. Unger, P.E. and Suuberg, E.M., 18th Symposium (Int) on Combustion, The Combustion Institute, Pittsburgh, PA, (1981), p. 1203.

47. Suuberg, E.M., Unger, P.E., and Lilly, W.D., Fuel, (1985), 64, 956.

48. Unger, P.E. and Suuberg, S.E., Fuel, (1984), 63, 606.

49. Oh, M.S., Peters, W.A., and Howard, J.B., AIChE J., (1989), 35 (5), 775.

50. Serio, M.A., Ph.D. Thesis, Department of Chemical Engineering, Massachusetts Institute of Technology, Cambridge, MA (1984).

51. Khan, M.R., Serio, M.A., Malhotra, R., Solomon, P.R., "A Comparison of Liquids Produced from Coal by Rapid and Slow Heating Pyrolysis Experiments", to be presented at the ACS Div. of Fuel Chem. Meeting, Miami, FL, (9/89).

52. Fong, W.S., Peters, W.A., and Howard, J.B., Fuel, (1986), 65, 251.

53. Solomon, P.R. and Carangelo, R.M., Fuel, (1982), 61, 663.

54. Solomon, P.R. and Carangelo, R.M., Fuel, (1988), 67, 949.

TABLE 1 - COMPARISON OF NETWORK MODELS

	CPD	DISARAY	FG-DVC Monte-Carlo or 2 σ	Relevant Model Process
Tar Yield vs Time	Yes	Yes	Yes	Bond breaking
Extract Yield vs Time	No[a]	No	Yes	Bond breaking
Gas Yield vs Time	Yes	Yes	Yes	From peripheral groups
Tar Yield vs Heating Rate	Not Yet	Yes	Yes	Relative rates of bond breaking and crosslinking
Variation of Tar Molecular Weight with Heating Rate	No	No	Yes	Relative rates of bond breaking and crosslinking
Molecular Weight of Tar	No	No	Yes	Mass transport Limitation
Tar Yields vs Pressure	No	No	Yes	Mass transport Limitation
Molecular Weight vs Pressure	No	No	Yes	Mass transport Limitation
Solvent Swelling of Char	No	No	Yes	Crosslinking

[a] All oligomers are defined as tar

- 128 -

Figure 1. Macromolecular Network Used in Monte Carlo Simulation.

Figure 2. Bethe Lattice for a) Coordination Number 2.2, p=1 and b) Coordination Number 4, p=1.

Figure 3. Percolation Theory Predictions for Pyrolysis Products (monomers, tar, extracts and total liquids) for Three Values of the Coordination Number $(\sigma + 1)$. a) $\sigma + 1 = 2.2$, b) $\sigma + 1 = 3.25$ and c) $\sigma + 1 = 4.6$.

Figure 4. Summary of Model Assumptions for a) Bridge Breaking, b) Crosslinking and c) Product Distribution.

Figure 5. Tar Yield for a Bituminous Coal Predicted by the CPD Model. a) Tar Yield vs. α, and b) Variation in α with Time Heating at 450°C/sec to 936 K. The Shaded Areas Show the Relative Amounts of the Two Types of Crosslinks (Initial; Unbreakable Bridge Formation).

Figure 6. Extract Yield for a Bituminous Coal Predicted by the FG-DVC Model. a) Extract Yield vs. α and b) Variation in α with Time Heating at 450°C/sec to 936 K. The Shaded Areas Show the Relative Amounts of the Three Types of Crosslinks (Initial; Crosslinks Related to Gas Evolution; Unbreakable Bridge Formation).

Figure 7. Extract Yield for a Lignite Predicted by the FG-DVC Model. a) Extract Yield vs. α and b) Variation in α with Time Heating at 450°C/sec to 936 K. The Shaded Areas Show the Relative Amounts of the Three Types of Crosslinks (Initial; Crosslinks Related to Gas Evolution; Unbreakable Bridge Formation).

Figure 8. Distribution of Hydrogen in Coal and Pyrolysis Products. Pyrolysis Produced Approximately 53% Char, 30% Tar and 21% Gas.

Figure 9. Comparison of Extract Yield Predictions from FG-DVC Model with Percolation Theory for σ = 1, 2, 3 and 4. FG-DVC Predictions are for Pittsburgh Seam Coal Heated at 450°C/sec to 936 K with No Tar Evolved.

Figure 10. Bethe Lattice for Two-σ Model with σ_1 = 1 (shown as single bonds) and σ_2 = 1 (shown as double bonds). a) Fully Linked Case (p= q = 1) is Like One-σ Model with σ = 3. b) Shown with Most Double Bonds (Representing the Crosslinks) Not Yet Formed to Represent the Starting Coal. This Lattice is Like a One-σ Model with σ = 1, Linear Chains.
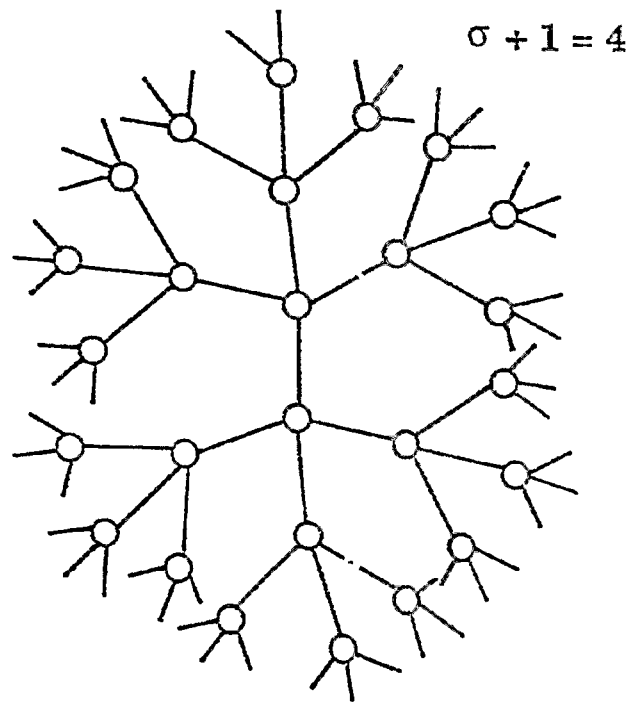
Figure 11. Comparison of Distribution of n-mers for Pyrolysis at 450°C/sec to 936 K. a) Monte Carlo Calculation, b) Two-σ Model (σ_1= 1, σ_2= 1), c) One-σ Model (σ =1.2) and d) One-σ Model, σ = 2.2.

Unbreakable Bridge

Crosslink

Chain of ℓ Monomers

a

$\sigma + 1 = 2.2$

b

$\sigma + 1 = 4$

a Bond Breaking

DISARAY

$$K_B = 6.8 \times 10^8 \exp(-30,000/RT) \; sec^{-1}$$

$$K_{tar} = 1.4 \times 10^7 \exp(-31,000/RT) \; sec^{-1}$$

CPD

$$K_B = 2.6 \times 10^{15} \exp(-55,400/RT) \; sec^{-1}$$

1.0

1.0

FG-DVC

$$K_B = 0.86 \times 10^{15} \exp(-55,400/RT) \; sec^{-1}$$

1.0

0.9

b <u>Crosslinking</u>

DISARAY

$$k_{char} = 2.0 \times 10^6 \exp -(24,600/RT) \text{ sec}^{-1}$$

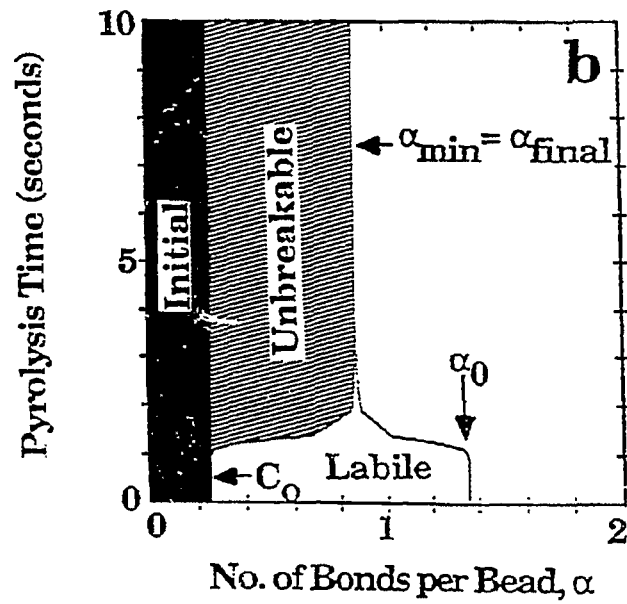$$k_{char} = 2.0 \times 10^6 \exp -(24,600/RT) \text{ sec}^{-1}$$
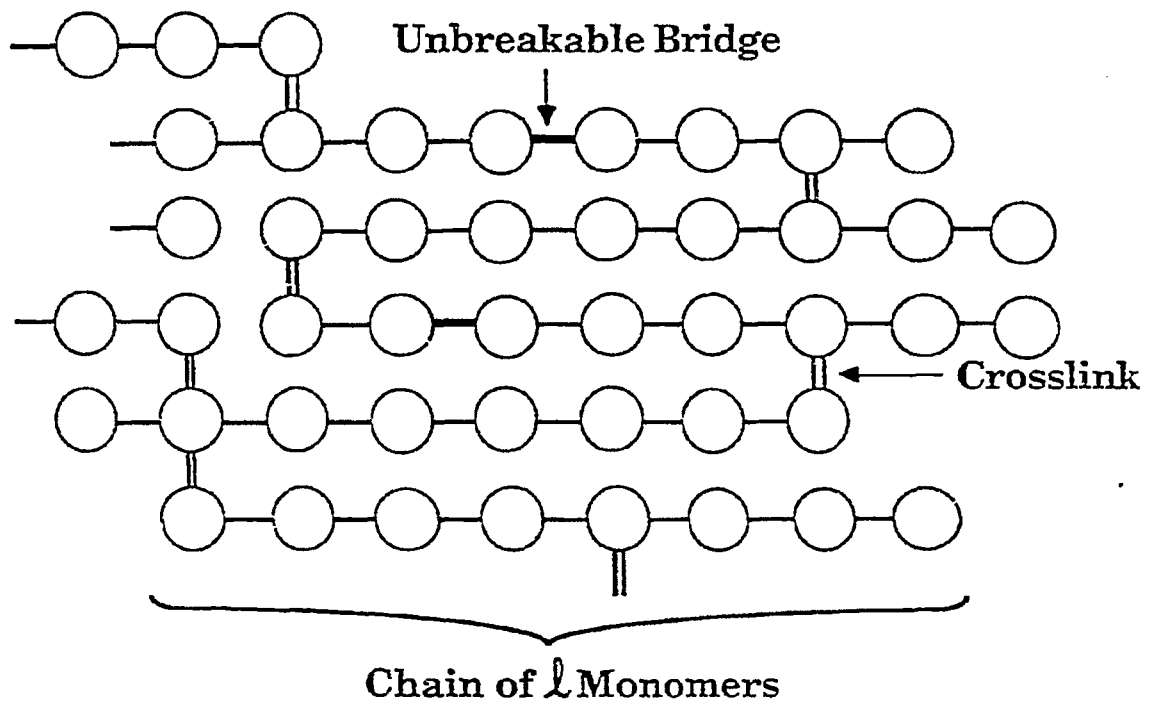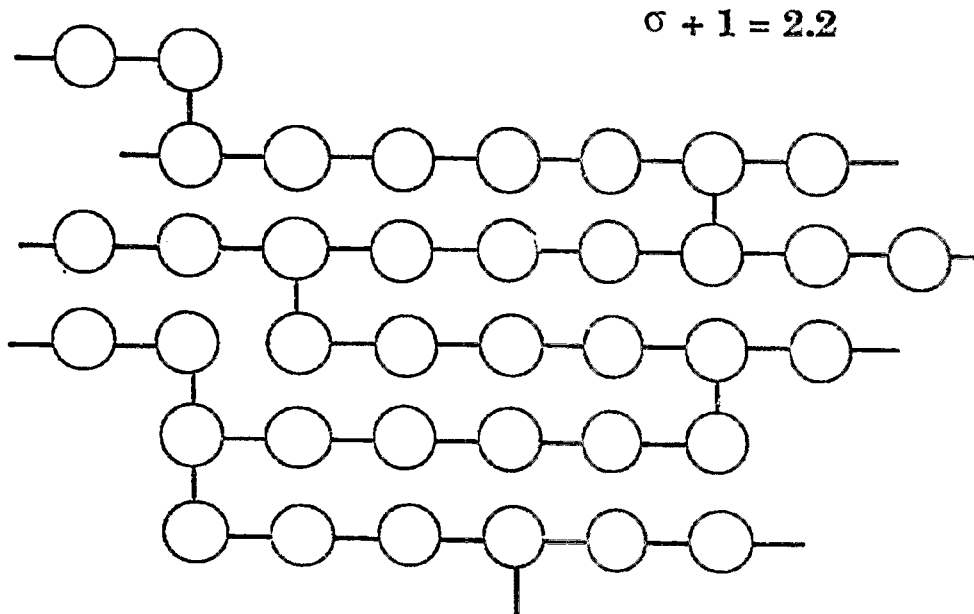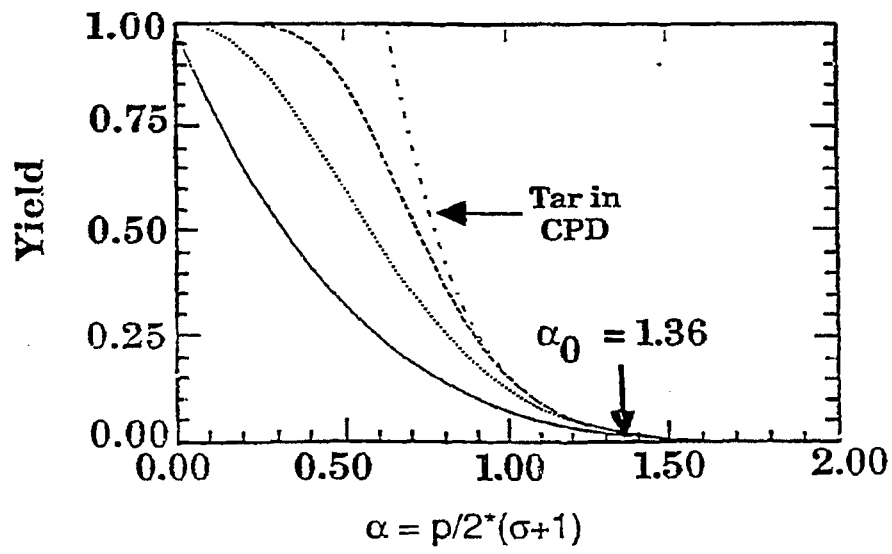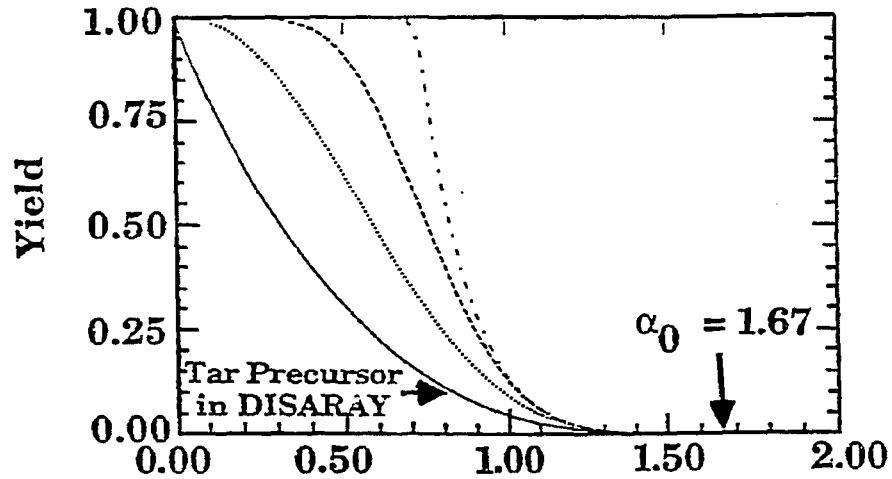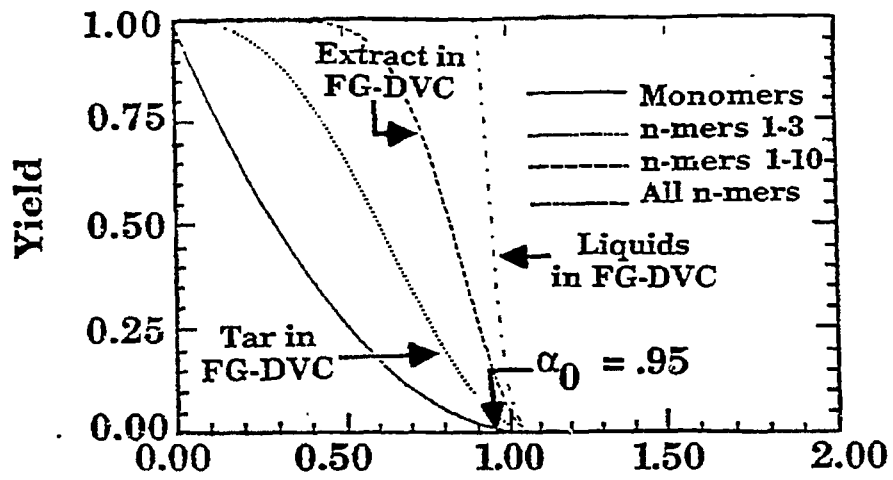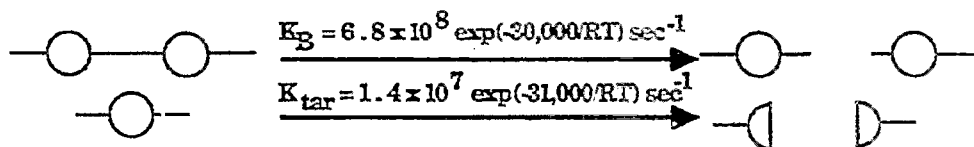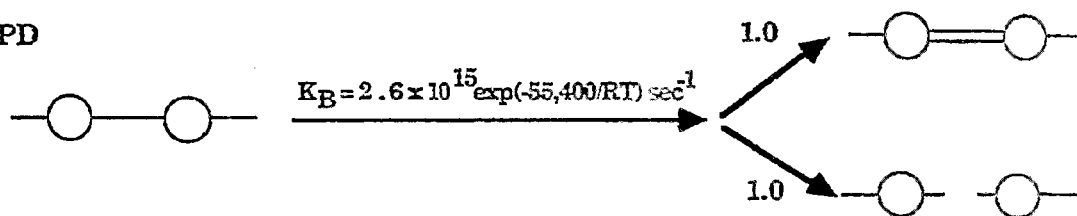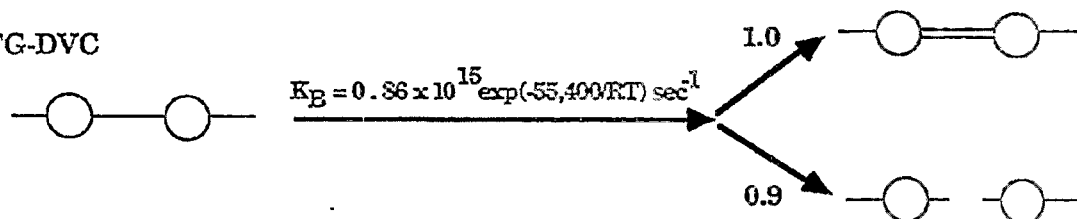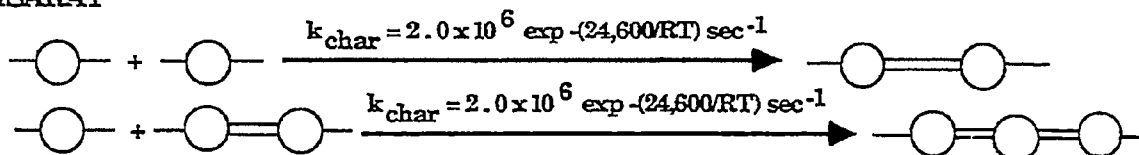
CPD

No Independent Crosslinking Process

FG-DVC

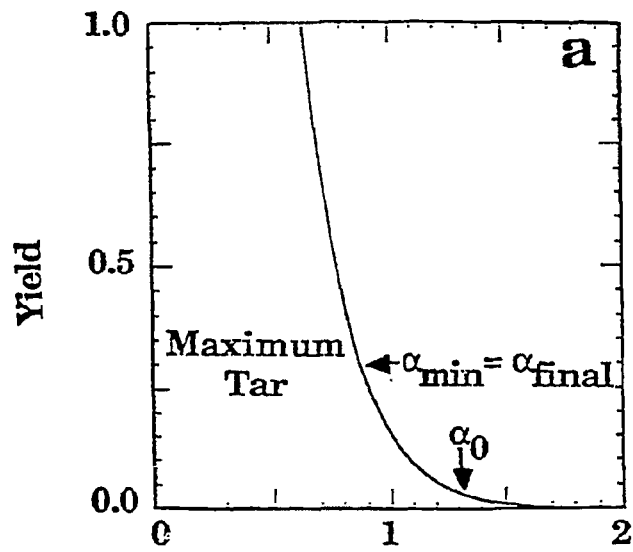$$k_{low} = 0.8 \times 10^{13} \exp(-45,000/RT) \text{ sec}^{-1}$$
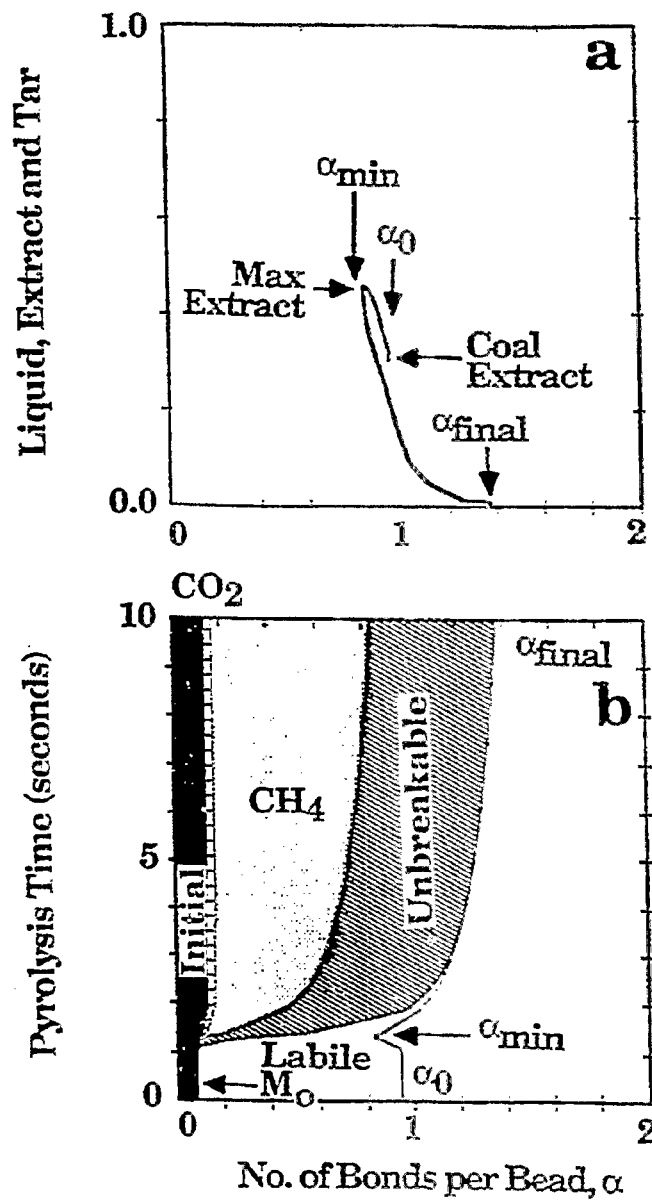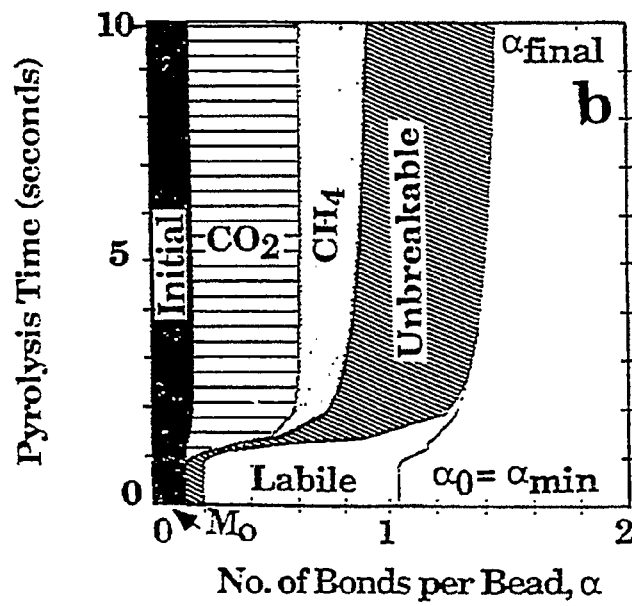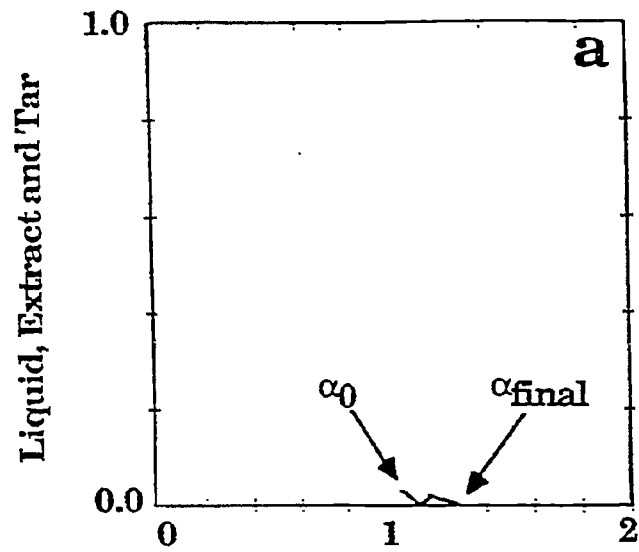
$$k_{mod} = 0.75 \times 10^{14} \exp(-60,000/RT) \text{ sec}^{-1}$$

c Product Distribution

DISARAY

CPD

FG-DVC

a

Yield

1.0

0.5

Maximum
Tar

$\alpha_{min} = \alpha_{final}$

α_0

0.0

0   1   2

b

Pyrolysis Time (seconds)

10

5

0

Initial

Unbreakable

$\alpha_{min} = \alpha_{final}$

α_0

C_0 Labile

0   1   2

No. of Bonds per Bead, α

Liquid, Extract and Tar

α_0 α_{final}

a

Pyrolysis Time (seconds)

α_{final}

b

Initial

-CO_2

CH_4

Unbreakable

Labile $\alpha_0 = \alpha_{min}$

M_0

No. of Bonds per Bead, α

Figure showing a bar chart of Weight % Hydrogen for Coal, Pyrolysis Product, Tar, and Char. Categories: Aromatic, Hydroxyl, Gas, Aliphatic.

Bar labels:
- Pyrolysis Product: .6 Tar, 1.7 Char, 1.35 Tar, .3 Char

X-axis labels: Coal, Pyrolysis Product, Tar (Wt.% of Tar), Char (Wt.% of Char)

Y-axis: Weight % Hydrogen, 0 to 8

Yield

1.00

0.75

0.50

0.25

0.00

2

3

4

$\sigma = 1$

α_{min}

α_0

α_{final}

0.00   0.50   1.00   1.50   2.00

$\alpha = p/2^*(\sigma+1)$

a

b

a

Product Distribution

All n-mers

900-3000 AMU

100-900 AMU

Temperature (°C)

b

Product Distribution

All n-mers

11-100

4-10

1-3

Temperature (°C)

c All → n-mers

Product Distribution

11-100

4-10

1-3

Temperature (°C)

d

Product Distribution
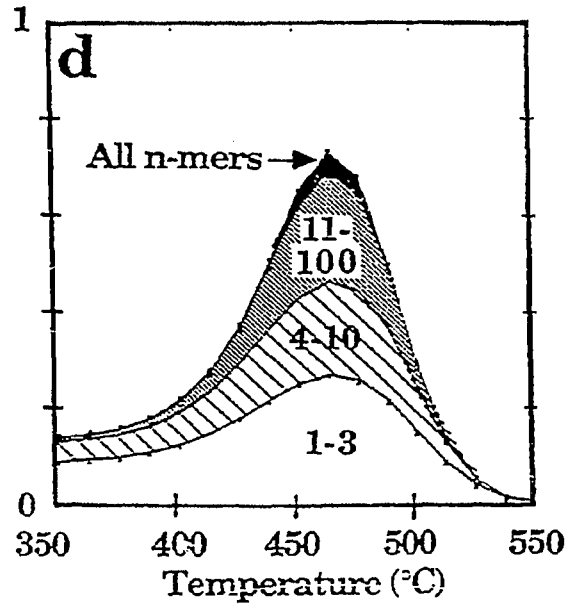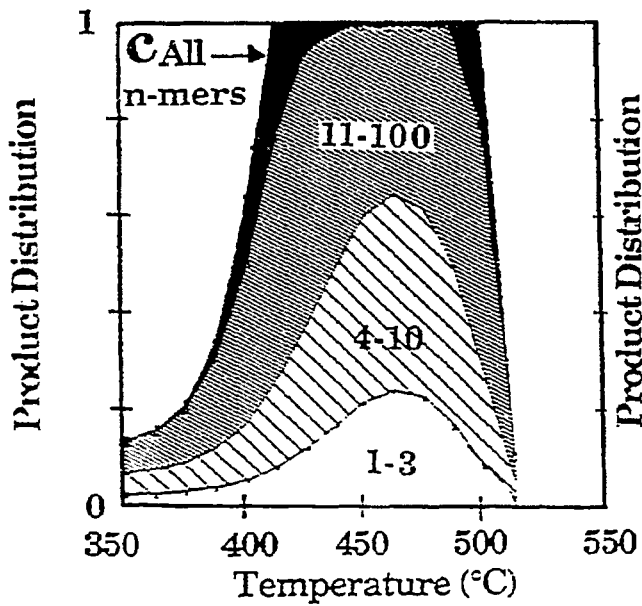
All n-mers →

11-100
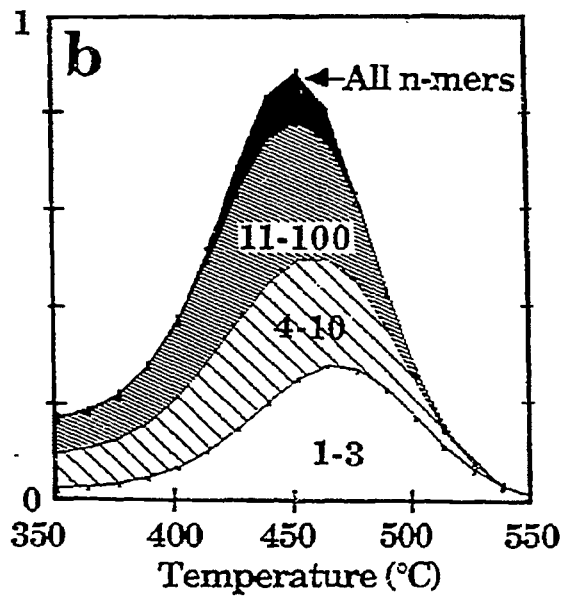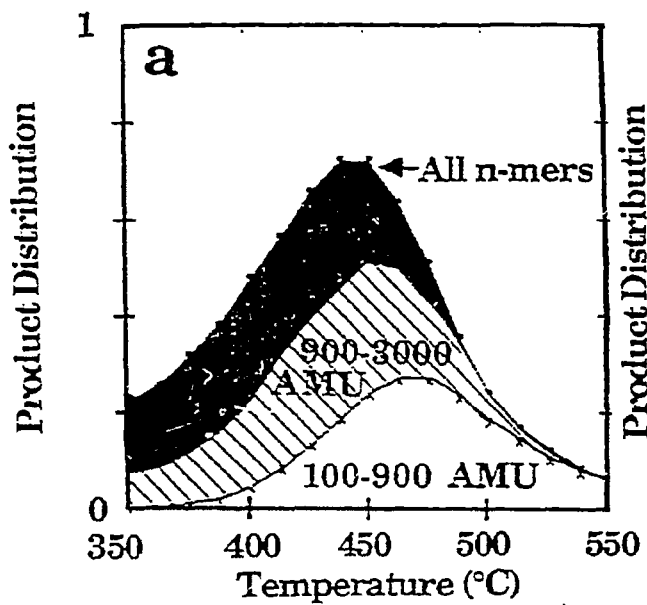
4-10

1-3

Temperature (°C)

APPENDIX A

The probability $F_{s,u}(p,q)$, that a site is a member of a cluster of n sites with s type 1 bridges and u type 2 bridges is given by

$$F_{s,u}(p,q) = a_{s,u} \, p^s \, (1-p)^\tau \, q^u \, (1-q)^\nu \tag{1}$$

where

$$
\begin{aligned}
n &= u + s + 1 \\
\tau &= (\sigma_1 + 1) \, n - 2s \\
\nu &= (\sigma_2 + 1) \, n - 2u
\end{aligned}
\tag{2}
$$

and τ, ν are the number of broken bridges of type 1 and 2, respectively, on the perimeter of the cluster, and $a_{s,u}$ is the number of different ways to form such a cluster. Following the same procedure used by Fisher and Essam, we can derive an expression for the configuration coefficient

$$a_{s,u} = \frac{(\sigma_1 + 1) \, (\sigma_2 + 1)}{(s + \tau) \, (u + \nu)} \; \Gamma \, (s + \tau + 1) \bullet \Gamma \, (u + \nu + 1) \bullet (u + s + 1) \tag{3}$$

where Γ is a gamma function. Note that for $u = 0$ (no type 2 bonds), this reduces to the quantity nb_n in Ref. (30). To determine the probability, $F_n(p,q)$ that a given site is a member of a cluster of n sites, i.e., the fraction of n-mers, we must sum Eq. 1 over all possible values of s and u that give an n-site cluster:

$$F_n(p,q) = \sum_{s=0}^{n-1} a_{s,u} \, p^s \, (1-p)^\tau \, q^u \, (1-q)^\nu \; ; \qquad u = n - s - 1 \tag{4}$$

The total fraction of sites, $F(p,q)$ in finite clusters is the sum over all s and u

$$F(p,q) = \sum_{s=0}^{\infty} \sum_{u=0}^{\infty} F_{s,u}(p,q) = \left(\frac{1-p}{1-p^*}\right)^{\sigma_1 + 1} \left(\frac{1-q}{1-q^*}\right)^{\sigma_2 + 1} \tag{5}$$

where p^* and q^* are obtained by finding the least roots of

$$p^* \, (1-p^*)^{\sigma_1 + 1} \, (1-q^*)^{\sigma_2 + 1} - p(1-p)^{\sigma_1 + 1} \, (1-q)^{\sigma_2 + 1} = 0$$

$$q^* \, (1-q^*)^{\sigma_2 + 1} \, (1-p^*)^{\sigma_1 + 1} - q(1-q)^{\sigma_2 + 1} \, (1-p)^{\sigma_1 + 1} = 0$$

$$\tag{6}$$

The critical point, where an infinite lattice begins to form (i.e., $F(p,q)$ begins to decrease) becomes a critical curve which divides the p-q plane into two regions. Note that for $q = 0$, the equations all reduce to the single σ case given in Ref. 30.